SPACE TELESCOPE SCIENCE INSTITUTE
Operated for NASA by AURA

Instrument Science Report STIS 2011-02(v2)

Effects of CTE Degradation on Cycle 18 Observations with the STIS CCD

W. Van Dyke Dixon
Johns Hopkins University, Baltimore, MD

31 May 2011

ABSTRACT

The charge-transfer efficiency (CTE) of the STIS CCD—the ability of the detector to move charge between adjacent pixels during readout—continues to decline. In this ISR, we explore the scientific impact of CTE effects on Cycle 18 observations. In coronagraphic imaging, CTE trails degrade the photometry and astrometry of objects beyond the brightest regions of the stellar PSF. In spectroscopy, CTE trails remove flux from the target spectrum. In both cases, trails from cosmic rays and hot pixels impart considerable noise to observations of faint targets. Tools to correct the photometry and astrometry of point sources are available, but they are not applicable to extended sources and do not reduce the noise imparted by CTE trails. A pixel-based CTE correction would address all of these concerns, but is not yet available for STIS.

Contents:

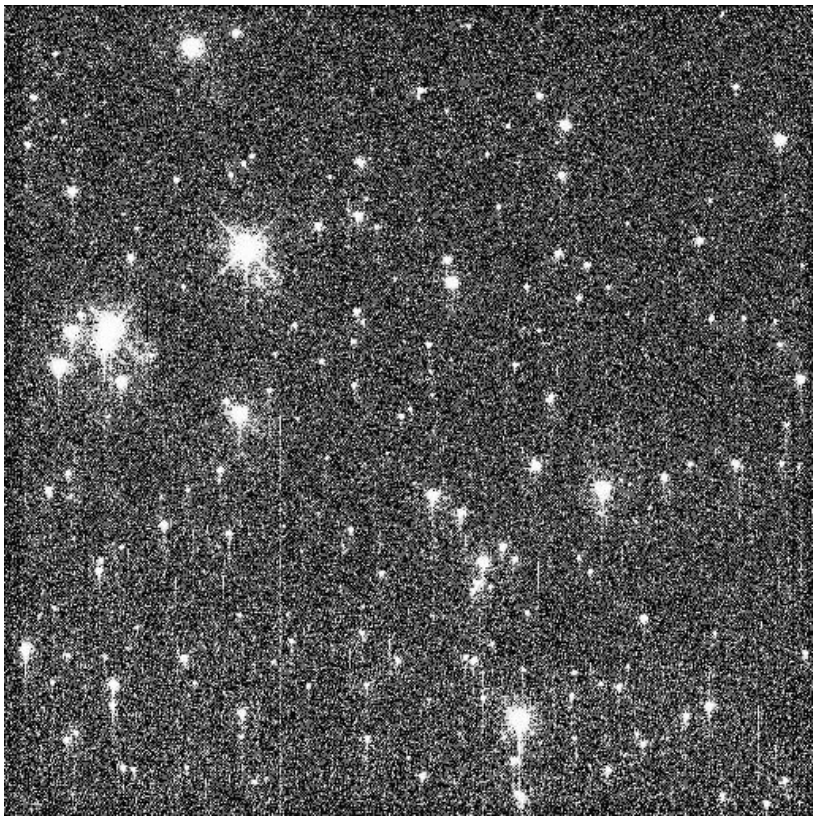

Figure 1. STIS CCD image of the globular cluster Omega Cen. Note the trails due to imperfect CTE. (Dataset obmj01050, 2011/02, Cycle 18, program 12409, PI: W. Dixon.)

1. Introduction

After more than 13 years on orbit, the STIS CCD detector shows the effects of accumulated radiation damage. In particular, its charge-transfer efficiency (CTE)—the fraction of charge successfully moved between adjacent pixels during readout—continues to decline. When this number is less than unity, some fraction of the stellar counts will trail behind the star in one or both dimensions of the image, as can be seen in Figure 1. A star whose counts must traverse many pixels before reaching the readout amplifier will appear fainter than a similar star close to the amplifier. For STIS, CTE losses are significant only in the parallel (Y) direction.

CTE trails have three effects. First, they remove counts from the data, reducing the observed flux in both spectroscopic and imaging observations. Second, they distort the images of stars and other targets, introducing a systematic bias into astrometric measurements. Third, the trails from cosmic rays and hot pixels that lie between the target and the read-out amplifier (down-stream trails) add noise to the data. In this ISR,

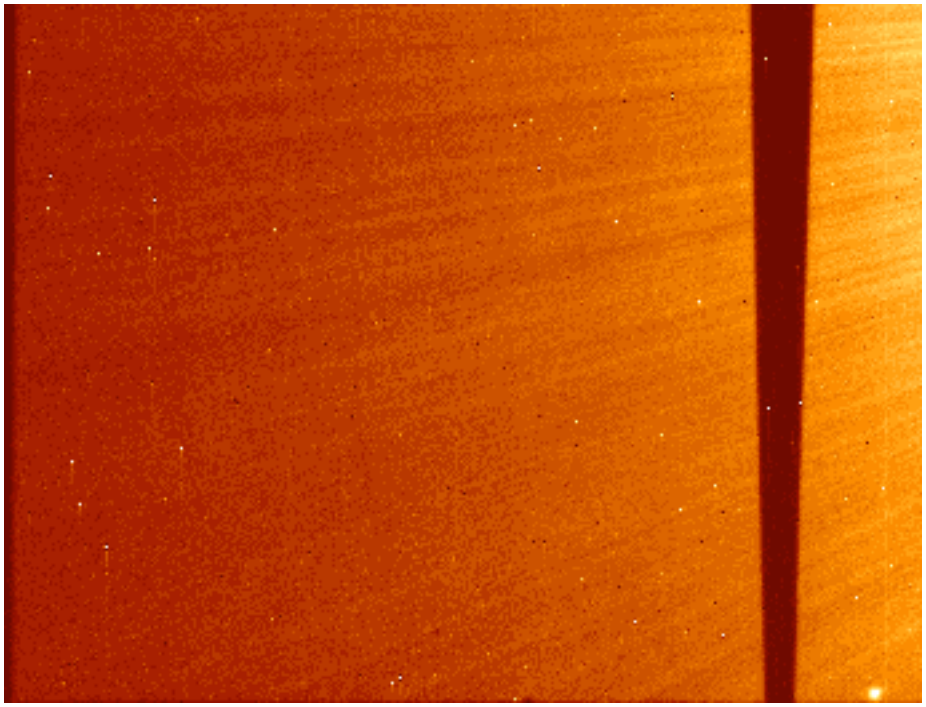

Figure 2. Coronagraphic image of the field around the star Fomalhaut, courtesy of Paul Kalas. Only a fraction (360 × 275 pixels) of the full (1024 × 1024 pixels) image is shown. The lower part of wedge A is visible; the star lies to the right of the image. CTE trails become increasingly apparent at greater distances from the star. (Dataset ob7919010, 2010/09, Cycle 16, program 11818, PI: P. Kalas.)

we discuss these effects and techniques for minimizing them.

2. Impact of CTE on STIS CCD Science

2.1 Cycle 18 Use of STIS CCD

In Cycle 18, STIS users were awarded 26% of all *HST* prime orbits. They are divided evenly among the three detectors, with the CCD receiving 35% of orbits. Of these, 45% are devoted to imaging (nearly all of which is coronagraphy) and 55% to spectroscopy. Two gratings are particularly popular: G430L receives 45% of the spectroscopic orbits, and G750M receives 42%. In total, 4% of *HST* prime orbits are devoted to coronagraphy and 5% to spectroscopy with the STIS CCD.

2.2 Impact of CTE on Coronagraphy

In recent observing cycles, most STIS CCD imaging has used the coronagraphic mask to study circumstellar disks and planets. When a bright star is placed behind the mask, the stellar point-spread function (PSF) extends across the field, filling the charge traps like a

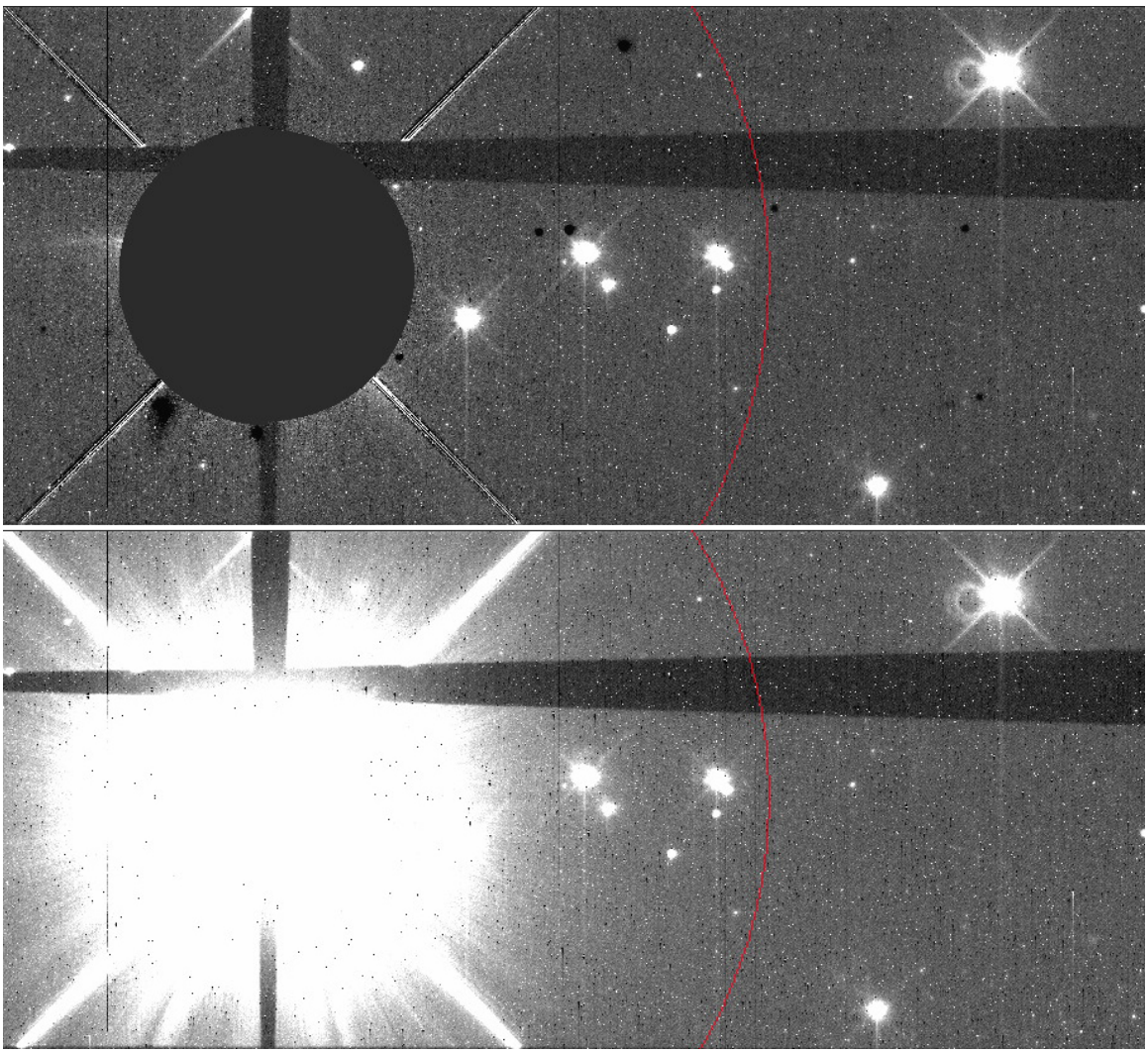

Figure 3. Coronagraphic image of a V = 8.2 mag star, courtesy of Glenn Schneider. The lower panel shows the field before subtraction of the stellar PSF. The upper panel shows the field after PSF subtraction. The black (filled) and red circles have radii of 6” and 20”, respectively. (From the Cycle 18 program 12228; PI: G. Schneider.)

pre-flash. Near the star, CTE effects are negligible; farther away, they begin to reappear.

Figure 2 presents a coronagraphic image of the field around the star Fomalhaut. The exposure was taken with CR-SPLIT=7; the images were combined to reject cosmic rays. The star lies at wedge position B2.5, about 33” to the right of the image center. (Compare with Figure 12.6 of Bostroem et al. 2010.) Hot pixels within about 20” of the star do not show CTE trails, but those farther away do. For reference, the median pixel value approximately 20” from the star is 200 electrons in each CR-SPLIT image.

At V = 1.16, Fomalhaut is unusually bright; for most targets, the CTE-free zone will be considerably smaller. For example, Figure 3 presents a deep exposure of the field around a V = 8.2 mag star from program 12228, which seeks to image circumstellar debris disks. The lower panel shows the field before subtraction of the stellar PSF. The upper panel, with an identical stretch, shows the field after PSF subtraction. The black circle (which obscures the target) has a radius of 6"; the red circle has a radius of 20". Around this object, CTE trails are apparent at radii much smaller than those around Fomalhaut.

The impact of CTE effects on coronagraphic observations thus depends on the scientific goals and target brightness. Circumstellar objects lying within the brightest part of the stellar PSF are essentially immune to CTE effects, while those farther out suffer the photometric and astrometric errors associated with imperfect CTE.

2.3 Impact of CTE on Spectroscopy

Down-stream trails due to cosmic rays and hot pixels can be a significant source of noise for spectroscopic observations. To investigate their impact, we consider two extremes: a pair of faint supernovae and a bright calibration star.

2.3.1 Faint Targets

We begin with the pair of faint (V = 18) supernova spectra plotted in Figure 4. Both were observed in late 2009 with grating G430L for a total of 2300 seconds using CR-SPLIT= 3, but one was placed at the center of the CCD (Y ~ 512, red), while the other was placed at the E1 position (Y ~ 900, black), closer to the read-out amplifier (Y = 1024; Bostroem et al. 2010, p. 133). The spikes in both spectra are CTE trails from down-stream cosmic rays and hot pixels. Though the two exposures were obtained under similar conditions, the red spectrum shows dozens more CTE trails than does the black.

Some simple statistics can help to quantify the noise imparted by CTE trails. We use the E1 (black) spectrum to construct a continuum model, removing hot pixels by hand and smoothing by 5 pixels, then divide both spectra by this model (scaling the red spectrum as necessary) to normalize them. The results are plotted in Figure 5. Our model does a reasonable job of normalizing both spectra at wavelengths beyond 4300 Å.

To compute the statistics, we use only the region between 4300 and 5600 Å, which is well behaved. We mask the 2-3 most discrepant pixels in each spectrum to keep them from dominating the results. The mean and standard deviation of the central (red) spectrum are $\mu = 1.16$ and $\sigma = 0.46$, corresponding to a mean signal-to-noise ratio (S/N) per two-pixel resolution element of 3.07 ($\mu/\sigma \times \sqrt{2}$). The corresponding values for the E1 (black) spectrum are $\mu = 1.00$, $\sigma = 0.09$, and S/N = 16.6.

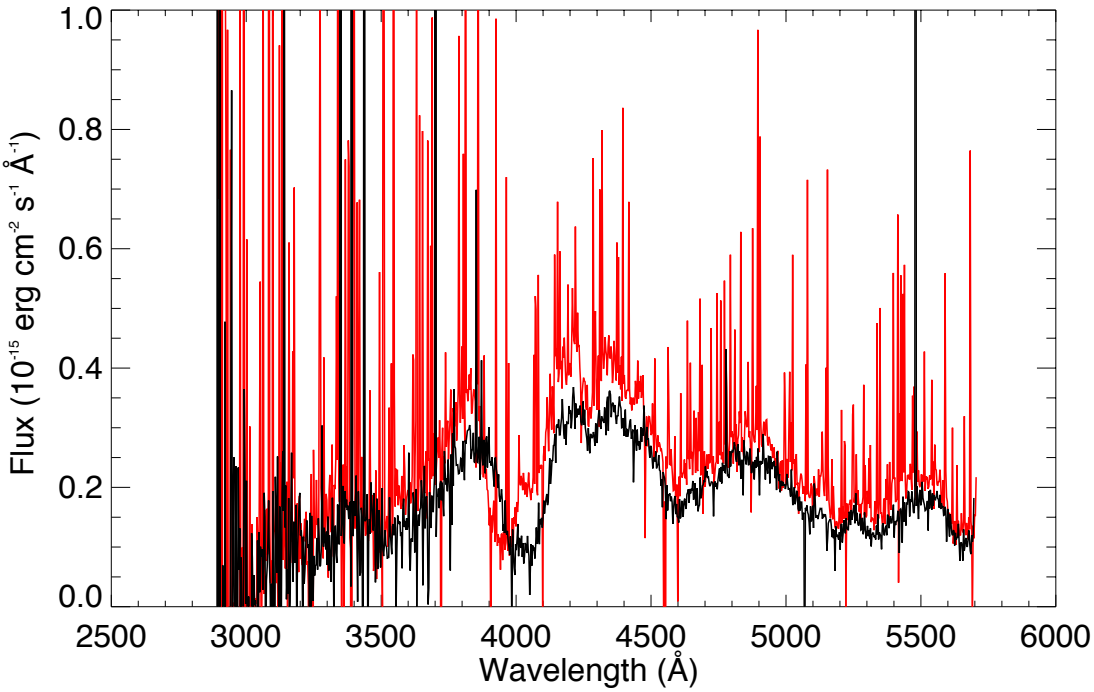

Figure 4. Spectra of two supernovae observed with the STIS CCD. The red curve (obd702010; 2009/09) was obtained at the center of the CCD and shows numerous CTE trails from down-stream cosmic rays and hot pixels. The black curve (obd704010; 2009/10) was obtained at the E1 position (Y ~ 900), closer to the read-out amplifier. (From the Cycle 17 program 11721, PI: R. Ellis.)

While use of the E1 position significantly reduces the noise due to CTE trails, it is not a panacea. When given our continuum model as input, the STIS Exposure Time Calculator (ETC) estimates that a 2300-second exposure with CR-SPLIT=3 would yield a spectrum with S/N between 25 and 45 per resolution element in this wavelength range. The mean S/N of the E1 spectrum is half this value. (Vignetting at the E1 position, discussed below, contributes ~ 10% of this discrepancy.) Faint CTE trails thus represent an important source of noise that is not included in the ETC.

The number of resolution elements affected by CTE trails represents a second measure of the CTE contamination. How many of the pixels in the central spectrum (red) differ from unity by more than 3 times the standard deviation of the E1 spectrum (black)? Of the 474 pixels between 4300 and 5600 Å, 94 (~ 20%) are discrepant in this way. Only 5 of the E1 pixels in this wavelength range are so discrepant.

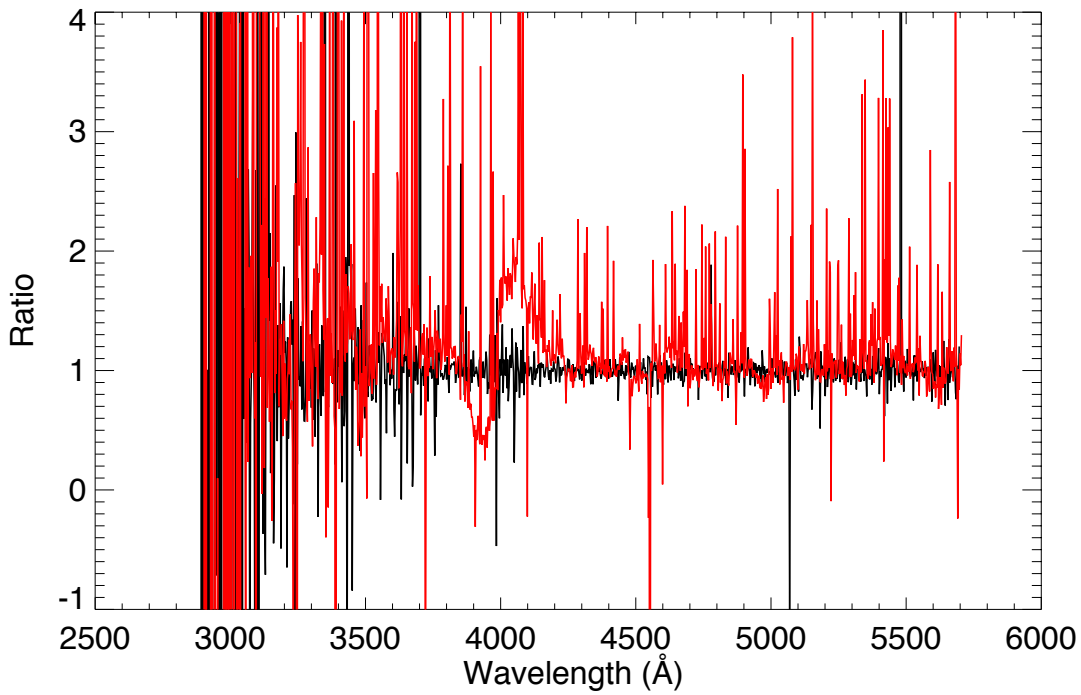

Figure 5. Spectra from Figure 4, normalized by a continuum model derived from the E1 (black) spectrum.

2.3.2 Bright Targets

CTE effects may be ignored if the target is bright enough. In 2010, the calibration star HIP 45880 (V = 12) was observed at a variety of positions along the 52X2 aperture. We consider two of these exposures, one obtained at the center of the chip (obau220b0) and one at the E1 position (obau220e0). Both have total integration times of 50 s and employ CR-SPLIT = 2 and the G430L grating. In Figure 6, the E1 spectrum is plotted in black and the central spectrum in red. Examination of the raw data frames shows the presence of miriad CTE trails, but only two noise spikes are apparent in the figure; both appear in the E1 (black) spectrum. (They may be due to hot pixels.) The combination of short exposures, which limit the number of cosmic rays, and bright spectra, which fill the charge traps, makes this target essentially immune to contamination by CTE trails. For this spectrum, the STIS ETC predicts a signal-to-noise ratio of 181.2 per two-pixel resolution element at 4451 Å; the measured value is 152.2 for the central spectrum and 134.7 for the E1 spectrum. The lower signal-to-noise ratio of the E1 spectrum reflects vignetting in the optical path. Because of this vignetting, the E1 position should not be used when the highest S/N ratios are desired.

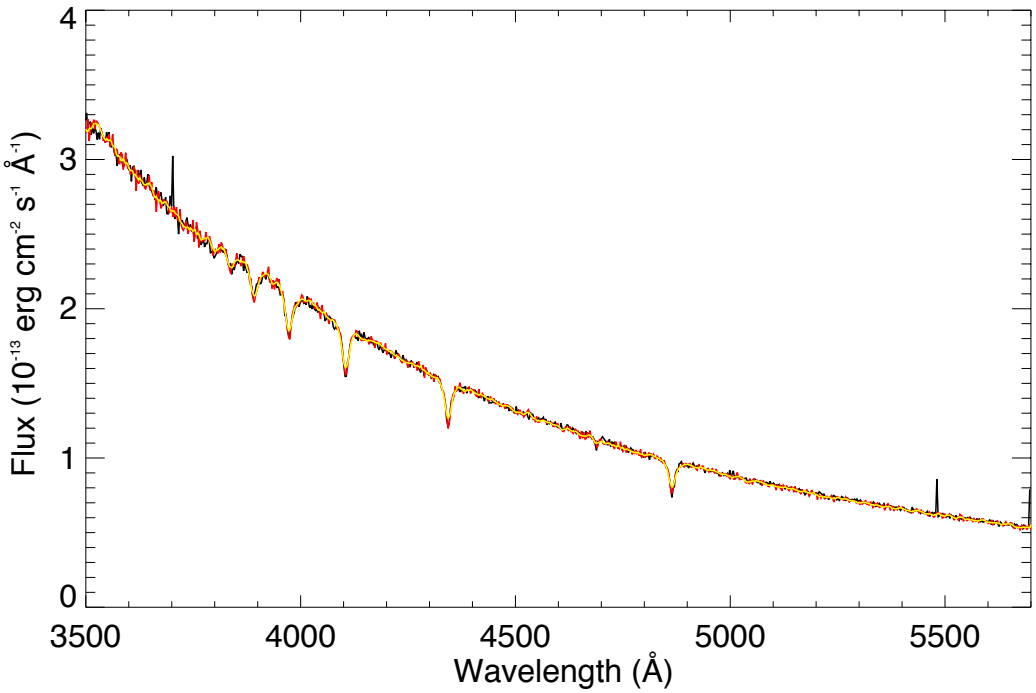

Figure 6. Spectrum of the bright star HIP 45880 observed with the STIS CCD. The red curve (obau220b0) was obtained at the center of the CCD. The black curve (obau220e0) was obtained at the E1 position. (2010/05, Cycle 17, program 11855, PI: C. Proffitt.)

2.4 Tools to Correct for CTE Effects

Goudfrooij et al. (2006) present algorithms for correcting the measured flux in the images and spectra of point-source targets for counts lost to imperfect CTE. These formulae reduce the systematic residuals due to CTE effects to within ~ 1.5% (RMS). A tool to correct STIS CCD photometry for CTE effects is available in the IRAF task **ccdstis**, and first-order CCD spectra are automatically corrected for CTE flux losses by the **calstis** data-reduction pipeline (Dressel et al. 2007).

Goudfrooij et al. (2006) also present a formula for correcting STIS CCD astrometry for the distortions introduced into stellar PSFs by imperfect CTE. This formula was recently incorporated into **ccdstis** (version Apr11), which now outputs a correction (in pixels) to be added to the measured Y centroid of each point-source target.

Note that all of these tools were developed for point-source targets; they cannot be used for extended sources, such as circumstellar disks or external galaxies. Also uncorrectable are the noise spikes imposed on both imaging and spectroscopic observations by the trails of down-stream cosmic rays and hot pixels. Pixel-based CTE correction algorithms, like those currently under development for *HST*/ACS (Anderson & Bedin 2010) would address both problems, but are not yet available for STIS.

3. Conclusions

The three principal consequences of imperfect CTE are photometric errors due to the loss of charge to CTE trails, astrometric errors due to the PSF distortions caused by these trails, and increased noise from the trails of down-stream cosmic rays and hot pixels.

Observers interested in STIS CCD coronagraphy should consider the location of the circumstellar disk or planet relative to the brightest region of the stellar PSF. Regions with scattered-light levels greater than about 200 electrons per pixel per exposure should suffer minimal CTE effects.

Observers who wish to obtain spectra of faint targets with the STIS CCD should place them at the E1 position, close to the read-out amplifier. The resulting spectra will suffer lower CTE flux losses and less contamination from down-stream trails. Even at the E1 position, however, faint CTE trails reduce the S/N of faint spectra by a factor of two relative to ETC predictions.

Techniques have been developed to correct for photometric and astrometric errors in imaging and spectroscopic observations of point-source targets, but they are not applicable to extended sources and do not address the noise imparted by down-stream CTE trails. A pixel-based CTE correction algorithm, which would amelioirate all of these problems, is not yet available.

Acknowledgements

Thanks to Paul Kalas, John Krist, and Glenn Schneider for helpful discussions regarding the impact of CTE effects on coronagraphic imaging; to Paul Kalas and Glenn Schneider for Figures 2 and 3 (respectively); and to Michael Wolfe for assistance with data analysis.

IRAF is distributed by the National Optical Astronomy Observatories, which are operated by the Association of Universities for Research in Astronomy, Inc., under cooperative agreement with the National Science Foundation.

Change History for STIS ISR 2011-02

Version 1: 20 May 2011 – Original Document

Version 2: 31 May 2011 – Clarify discussion of Figure 2.

References

Anderson, J. & Bedin, L. R. 2010, PASP, 122, 1035
Bostroem, K. A., et al. 2010, "STIS Instrument Handbook," Version 10.0 (Baltimore: STScI)
Dressel, L., et al. 2007, "STIS Data Handbook," Version 5.0 (Baltimore: STScI)
Goudfrooij, P., Bohlin, R. C., Maíz-Apellániz, J., & Kimble, R. A. 2006, PASP, 118, 1455